Analysis of Predictive Control for Boost Converter in Power Factor Correction Application

Arthur G. Bartsch, Christian J. Meirinho, Yales R. de Novaes, Mariana S. M. Cavalca, José de Oliveira
Department of Electrical Engineering
Center of Technological Sciences
University of State of Santa Catarina
Joinville, SC, Brazil, +55 47 3481-7846
Email: {arthurbartsch,christianmeirinho}@gmail.com,{yales.novaes,mariana.cavalca,jose.oliveira}@udesc.br

***Abstract*— This work presents a boost converter design methodology for active power factor correction, using finite control set model-based predictive control (FCS-MPC) for current control. Moreover, an external proportional integrative (PI) voltage control loop design methodology is explained. This paper also compares the conventional PI current control with MPC current for this application, both in transient load disturbance condition and in steady state different load conditions. The results in rated operation are compared with IEC 61000-3-2 international standard, which establishes limits for current harmonics rms values. The design methodology shows itself effective, with results near to the expected. Both controllers presented advantages and disadvantages, many of them exhaustively discussed in this work.**

I. Introduction

A constant preoccupation of industrial equipment producers is to attend international standards on total harmonic distortion (THD) and power factor (PF), specially, in order to sell for markets subjected to standards as IEC 61000-3-2 [1]. This norm establishes limits for current harmonic levels in equipment with input current lower than 16 A.

The main problem is that industrial and domestic equipment use power converters for developing DC sources or motor drives. The power converters are nonlinear loads which produce distortions in input current distortions that increases the harmonic current levels considerably in the location electrical grid. The high level of harmonic current implies on low power factor, electromagnetic compatibility problems, overload of the electric system, transformer saturation and other issues.

One of the worst power converters in terms of THD is the full-bridge monophase rectifier with capacitive filter [2]. A comparative between the norm patterns and the converter (1500 W) is presented in Figure 1.

In Figure 1, the need to perform a power factor correction (PFC) in this equipment shows itself obvious. There are two lines of PFC techniques: passive correction and active correction.

Passive correction reduces the harmonic content of the input current adding an inductor or a low pass LC filter in the converter input. However, these technique sometimes cannot attend the norm and, when it does, it occurs only near to the rated power of the rectifier.

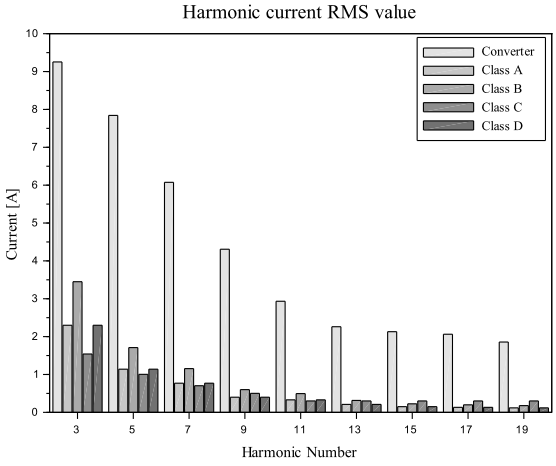

Fig. 1. Harmonic currents comparative of 1500 W monophase rectifier and IEC standard

In other hand, active PFC uses a controlled converter to power factor correction. This condition allows high power factor in a large range of operation and still guarantees the correct output voltage, even with disturbances in voltage grid [3], [4].

The main converter used for active PFC is the boost DC-DC converter, operating in any conduction mode (continuous, critical or descontinuous) [4].

For controlling the converter, usually a proportional-integrative (PI) controller is employed, in a cascade loop configuration. There is an internal and fast current loop and an external and slow voltage loop [3], [4].

Recently, many predictive control strategies have been tested for several applications in power electronics, including PFC. The main predictive strategy used in this applications is the finite control set model-based predictive control (FCS-MPC) due to its implementation simplicity, properly developed for power electronics [5]. In this technique, there is the treatment of commutation nonlinearity, which makes this technique very attractive. In active PFC with Boost converter, there are, in literature, experimental results of its appliance and validity [6].

However, the FCS-MPC has an awful issue for power converters project: the control has variable frequency operation, limited to the half of the sample time [7]. It implies on many difficulties to design the passive components of the converter and even to design the external voltage loop.

Considering this condition, many works, in active PFC applications have opted for use continuous control set model-based predictive control (CCS-MPC). This predictive strategy models the converter considering a duty cycle as the control action. In the active PFC, there are some works with this control strategy [2], [4], [8]–[10].

This work main objective consists in to develop a design method for the boost converter, to apply the FCS-MPC with the maximum current THD reduction and low voltage ripple. The results are compared with the traditional PI controller strategy.

In Section II, the FCS-MPC fundamentals are presented. In Section III, the converter and the control design for predictive control technique is shown. In Section IV, the converter and the control design for PI application are made. Simulated results are presented in Section VI. Finally, the conclusions are done in Section VII.

II. Predictive Control Fundamentals

Model-based predictive control was developed in petrochemical industry in the end of 1970 decade [11]. Posteriorly, the research in academy formalized this digital control strategy theory, culminating in several control techniques with the same principles [12].

Often, these techniques have some common aspects as the prediction model and the cost function. The prediction model is used to predict the future behavior of the plant, inside a prediction horizon (number of plant future steps predicted). The cost function is used to choose the control action to be applied in the process. The control action is calculated by minimizing the cost function, which weights costs of the system, like tracking errors, control action variation and other parameters [7], [12].

For power electronic converters, FCS-MPC can be easily used [5], [13]. In this predictive control strategy, treatment of commutation states non linearity is made, considering the future state of all converter switches. In the sequence, a cost function is evaluated. The state which implies lower cost is chosen to be applied to converter switches [5].

This technique has the advantage of treating multiple inputs multiple outputs (MIMO) systems, to treat process constraints directly in cost function, without saturation, to do not be dependent of an operation point of the system among others [5].

A. Prediction Model

Considering a boost converter, for inductor current control, operating in continuous conduction mode (CCM), there are two stages of operation.

In the first stage, the switch is active. Thus [3]:

$$i_L[k+1] = i_L[k] + \frac{t_s}{L} v_{in}[k]. \tag{1}$$

In the second stage, the switch is inactive and $i_L > 0$. Thus:

$$i_L[k+1] = i_L[k] + \frac{t_s}{L}(v_{in}[k] - v_{out}[k]). \tag{2}$$

Equations (1)-(2) describe the behavior of a future step of the current. It is enough for a FCS-MPC with unitary prediction horizon, which will be used in this work (it means the model is predicted one step in the future).

Due to (1)-(2), to evaluate this model, three sensors are necessary: an input voltage sensor (possibly, a resistive divider), an output voltage sensor (similar to previous case) and a current sensor (possibly, a shunt resistor).

B. Cost Function Analyzed and Optimization Process

The cost function analyzed in the proposed control has only one main objective: to track a current reference. Thus [5],

$$w(k) = |i^*[k+1] - i_L[k+1]| \tag{3}$$

where $i^*[k+1]$ is the future current reference, given by the external voltage loop.

The optimization process consists in to evaluate the cost function in the case with switch active and the cost with the switch inactive. The state with lower cost is chosen to be applied in the system.

For example: consider that in a given instant k the current reference i^* is 5 A, $i_L[k] = 4.8$ A, t_s = 0.1 ms (t_s is the controller sampling time), L = 10 mH, v_{in} = 70 V and v_{out} = 120 V. The control will calculate the $i_L[k+1]$ using (1) and will obtain that $i_L[k+1] = 5.5$ A. After, the control will calculate $i_L[k+1]$ using (2) and will obtain that $i_L[k+1] = 4.3$ A. Using (3), the cost of to active the switch is 0.5 A and the cost of to block the switch is 0.7 A. Therefore, the controller will choose to active the switch, since this condition has lower cost.

III. System Design with Predictive Controller

Considering the presence of current predictive controller, the design methods for the converter and the voltage external loop are presented in this section.

A. Converter Design

Table I presents the design criteria of the simulated boost converter.

A disadvantage of finite control set predictive controllers is the operation in variable switching frequency. As there is not a modulation with a fixed switching frequency, the design of converter passive elements is hard to make.

TABLE I
Boost Converter Design Criteria

Parameter	Value
V_{in}	220 V
V_{out}	450 V
ΔV_{out}	1.5%
P_{out}	1500 W
THD	3%

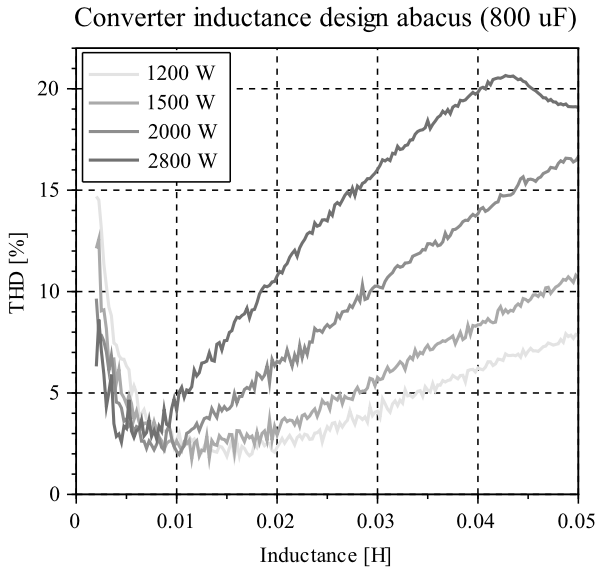

Fig. 2. Abacus for THD evaluation

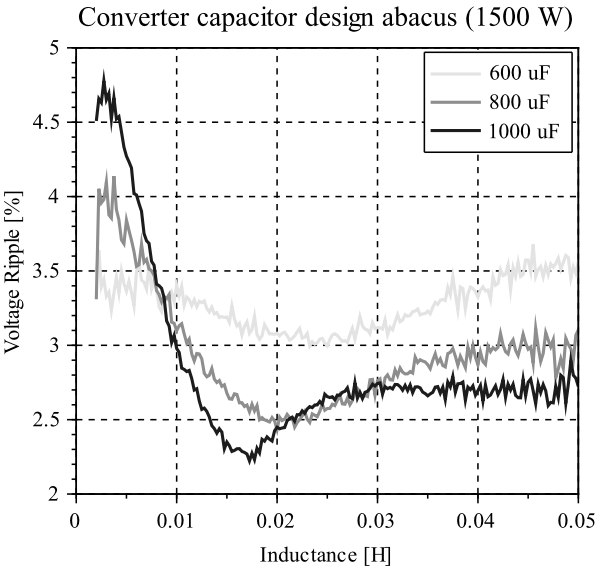

Fig. 3. Abacus for output voltage ripple evaluation

Due to this condition, an abacus was developed to help in the converter design, in terms of expect total harmonic distortion (THD) in function of inductance value and the converter power. The output capacitance has minimal influence in the curves of the abacus. Figure 2 presents the abacus for THD evaluation.

Another abacus was developed to help with the converter design in relation to the output voltage ripple. It was plotted in function of inductance value, for different capacitance values and convert power values. Output power has minimal influence on the ripple curves of the abacus. Figure 3 presents the abacus for capacitor design.

These abacus were developed as contribution of this work. In the process of the elaboration of the abacus, a current closed loop with predictive control, with a current reference as input was considered. The power curves was obtained varying the amplitude of the current reference. A sinusoidal wave (220 V) was considered as the phase input voltage in the converter. Moreover, the THD calculated considers fundamental frequency of 60 Hz (same of the input voltage). The sample time considered was 0.5 ms.

These abacus facilitate the design of the converter. The first abacus (Fig. 2) allows to choose a inductance range to reduce the THD, in function of the converter power. To determine the capacitance value, it is necessary to utilize the second abacus (Fig. 3), using the output voltage ripple as the design criteria. For this criteria, there are influences from the capacitance and the inductance. Therefore, it is possible to select the capacitance and the inductance that attends the voltage ripple criteria (obviously, respecting the THD criteria). The second abacus has low influence of the voltage converter. Logically, when there is an external voltage control loop, the THD index will have a small augment while the voltage ripple will reduce.

Then, applying this methodology, it is possible to determine the passive elements of the boost converter, to apply the MPC current control. Considering the output power equals to 1500 W, the inductance values among 5 mH and 20 mH generate a THD lower than 4%, as seen in the first abacus (Fig. 2). After establish the inductance range, it is possible to analyze the second abacus (Fig. 3). In the chosen inductance range, in the curve with capacitance equals to 1000 μF, it is possible to see that for values among 12.0 mH and 20 mH, the voltage ripple is lower than 2.5%. This the chosen values of inductance and capacitance are: L = 14.5 mH and C = 1000.0 μF.

B. Voltage Loop Control Design

For voltage control loop, it is proposed to use a numerically identified model. To get this model, it is used the plant output response for a given input. With the input and the output data, a least squares algorithm can be used to obtain the model parameters [11], [14].

Thus, applying this procedure, a step in current reference was applied and the voltage response was analyzed.

The model is given by:

$$v_{out}[k+1] = a_g v_{out}[k] + b_g i^*[k] \tag{4}$$

where a_g and b_g are the model parameters and i^* is the current reference, in a discrete time k. This way, $a = 0.9989427$ and $b = 0.0430124$ for $t_s = 0.5$ ms. In continuous frequency (s-plane), the model is given by:

$$\frac{V(s)}{I^*(s)} = \frac{k_g}{s + p_g} \tag{5}$$

with k_g=86.02 V/(As) and p_g = 2.11 rad/s.

Using frequency response method, a proportional-integrative control was designed. The controller zero was placed at two times the plant pole value. The open-loop

cut-off frequency was placed at 1.0 Hz (for minimize voltage loop influence in the current THD). Therefore, the proportional gain k_p = 0.096 A/V and integrative gain k_i = 0.404 A V^{-1} s^{-1}. These gains are valid for a continuous PI controller, but, as the switching frequency is very high they were also valid for the employed digital controller. Note that the digital PI controller is given with:

$$i^*[k] = k_p(v^*[k] - v_{out}[k]) + k_i \sum_{k_\xi=0}^{k} (v^*[k_\xi] - v_{out}[k_\xi])t_s \quad (6)$$

where v^* is the voltage reference and k_ξ is a counter.

IV. System Design with PI Controller

In this Section, the active PFC system design is presented considering a system with two PI loops in the cascade structure.

A. Converter Design

Considering the input v_{in} as the absolute value of a sinusoidal curve, it is possible to define the voltage factor α as:

$$\alpha = \frac{V_{in,p}}{V_{out}} \quad (7)$$

where $V_{in,p}$ is the peak voltage of input voltage and V_{out} is the mean value of output voltage.

This way, the inductance can be calculated as:

$$L = \begin{cases} \dfrac{V_{in,p}}{\Delta I_L f_s}(1-\alpha) & \text{if} \quad \alpha < 0.5 \\ \\ \dfrac{V_{out}}{4\Delta I_L f_s} & \text{if} \quad \alpha > 0.5 \end{cases} \quad (8)$$

where ΔI_L (in ampere) is the maximum current ripple.

The output capacitance is given by:

$$C = \frac{P_{out}}{2\pi f V_{out} \Delta V_{out}} \quad (9)$$

where P_{out} is the load power, f is the grid frequency and ΔV_{out} is the output voltage ripple.

Adopting the methodology above, considering $\Delta I_L = 0.5$ A and $\Delta V_{out} = 6$ V, the values of $L = 10$ mH and $C = 1.65$ mF are obtained.

B. Control Design

For the control design, there are two schemes: internal current scheme and external voltage scheme.

The internal current loop is done considering the simplified current per duty cycle plant [3]:

$$\frac{i(s)}{d(s)} = \frac{V_{out}}{sL} \quad (10)$$

where d is the duty cycle. This model is valid for high frequency aspects and help to design the proportional gain of the controller. After that, it is just necessary a small integrative gain, to put the controller zero near to PI origin pole. This way, for a 5 kHz open-loop cut-off frequency, $k_{p,i}$ = 1.5 A^{-1} and $k_{i,i}$ = 0.05 $A^{-1}s^{-1}$.

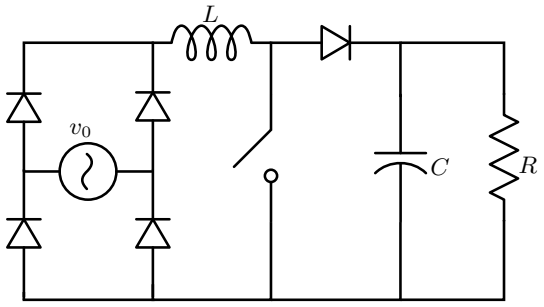

Fig. 4. Simulated Converter

For the voltage control loop, it was considered the model given by:

$$\frac{v(s)}{i(s)} = \frac{D/C}{s + RC} \quad (11)$$

where D is the mean duty cycle value.

For this model, it was established a 6 Hz open-loop cut-off frequency. The voltage controller zero is used to cancel the plant pole. Thus, $k_{p,v}$ = 0.15 A V^{-1} and $k_{i,v}$ = 0.9 A $V^{-1}s^{-1}$.

V. System Modeling

A simulation platform was developed in C language to emulate the non controlled rectifier with boost converter for improving power factor. Figure 4 exhibits the simulated converter.

Two simulation models were developed: one for the non controlled rectifier and other for the boost converter. All the system operates in closed loop. All semiconductors were considered ideal. Load disturbances were included in the simulation system.

A. Rectifier model

The full bridge diodes rectifier was modeled as an absolute value function. This way

$$v_{in}(t) = \begin{cases} v_0(t) & \text{if} \quad v_0(t) >= 0 \\ -v_0(t) & \text{if} \quad v_0(t) < 0 \end{cases} \quad (12)$$

where v_{in} is the input voltage of boost converter and v_0 is instantaneous voltage of the input source.

B. Boost converter model

The boost converter model for simulation was done using the operation stages [3].

In the first stage, the switch is active, thus

$$v_L(t) = v_{in}(t) = L\frac{di_L}{dt} \quad (13)$$

$$i_C(t) = -i_{out}(t) = C\frac{dv_C}{dt}. \quad (14)$$

In the second stage, the switch is inactive, with $i_L(t) > 0$. This way,

$$v_L(t) = v_{in}(t) - v_{out}(i) = L\frac{di_L(t)}{dt} \quad (15)$$

$$i_C(t) = i_L(t) - i_{out}(t) = C\frac{dv_C(t)}{dt}. \quad (16)$$

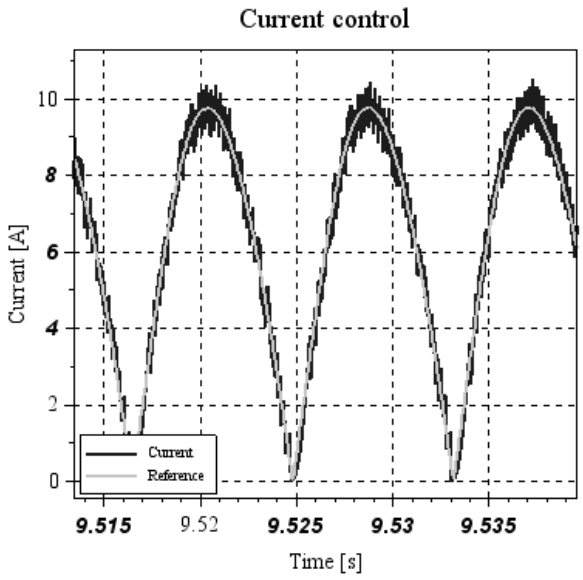

Fig. 5. Current reference tracking with FCS-MPC

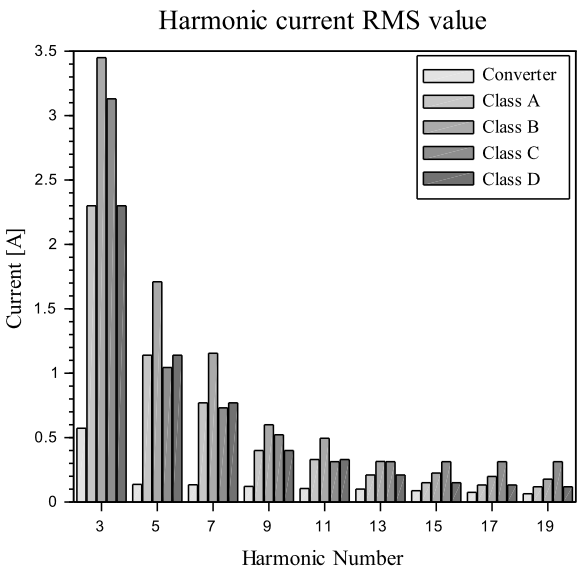

Fig. 6. Current harmonics comparison with IEC 61000-3-2 with FCS-MPC

Finally, if the converter operates in a discontinuous current mode, there is a third stage. In this stage:

$$v_L(t) = 0 \tag{17}$$

$$i_L = 0 \tag{18}$$

$$i_C(t) = -i_{out}(t) = C\frac{dv_C(t)}{dt}. \tag{19}$$

Table II presents all main parameters used in the simulations.

TABLE II
MAIN PARAMETERS SIMULATION

Parameter	Value	Parameter	Value
Simulation step	10^{-6} s	L with MPC	14.5 mH
Simulation total time	10 s	C with MPC	1.0 mF
Simulation minimum time	9,5 s	L with PI	10.0 mH
Points evaluated	50000	C with PI	1.65 mF
Control sampling time	500 μs	Output Power	1500 W
PI switching frequency	20 kHz	V_{out}	400 V
MPC max. switching frequency	10 kHz	$V_{in,p}$	311 V
Voltage PI (MPC) k_p	0.096	V. PI (MPC) k_i	0.404
Current PI $k_{p,i}$	1.5	C. PI $k_{i,i}$	0.05
Voltage PI $k_{p,v}$	0.15	V. PI $k_{i,v}$	0.9

VI. SIMULATION RESULTS AND DISCUSSION

This Section presents the simulation results of both evaluated active PFC systems. In both simulations, a load disturbance is considered (reduced from 100% to 50%).

A. PFC with current MPC

Figure 5 presents the current reference tracking with FCS-MPC controller.

Figure 6 presents the current harmonics, comparing with the values established by IEC 61000-3-2 [1].

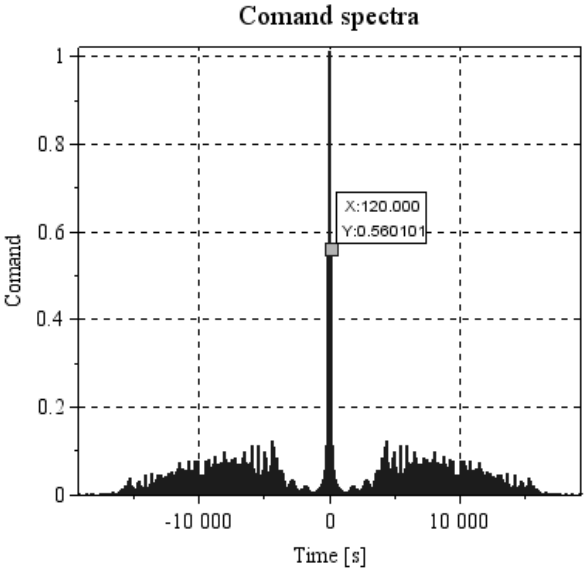

Fig. 7. Command frequency spectra with FCS-MPC

Figure 7 presents command spectra using FCS-MPC for control and modulation.

Figure 8 presents the voltage transient with load disturbance.

B. PFC with PI controller

Figure 9 presents the current reference tracking with PI controller.

Figure 10 presents the current harmonics, comparing with the values established by IEC 61000-3-2 [1].

Figure 11 presents command spectra using FCS-MPC for control and modulation.

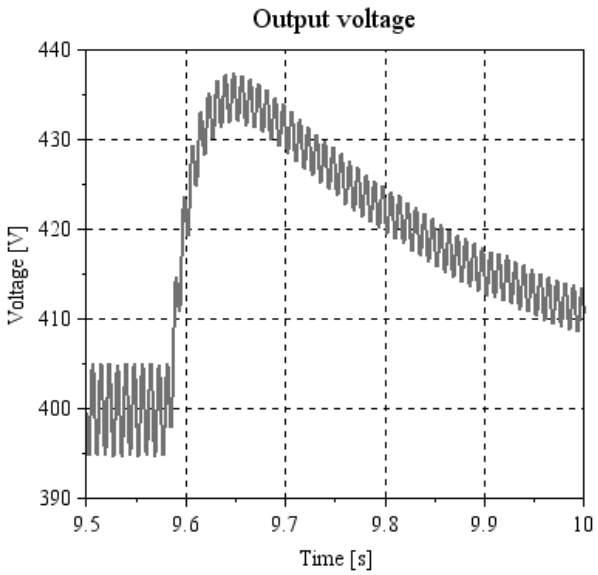

Fig. 8. Voltage transient with load disturbance with FCS-MPC in internal loop

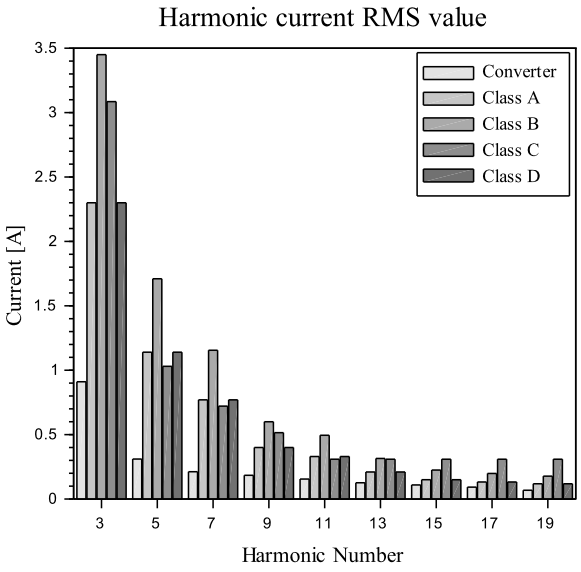

Fig. 10. Current harmonics comparison with IEC 61000-3-2 with PI

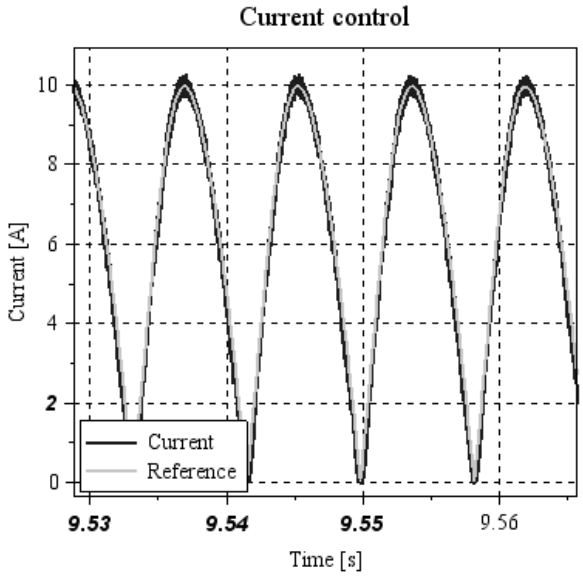

Fig. 9. Current reference tracking with PI

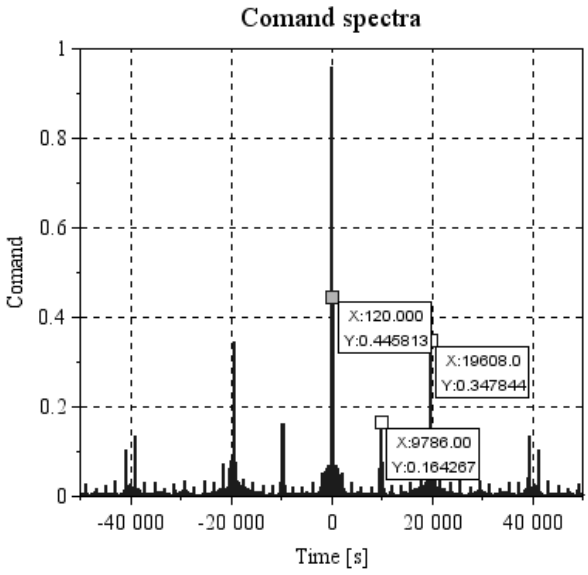

Fig. 11. Command frequency spectra with PI

Figure 12 presents the voltage transient with load disturbance.

C. Discussion

Table III presents the THD value for different load conditions, in steady state, comparing PI current controller and FCS-MPC current controller.

Figure 13 presents the comparison of i_0 (current on the sinusoidal source) using PI controller and using the MPC. In detail, the zero crossover is shown.

Figure 14 exhibits the comparison of i_0 harmonics between PI controller and MPC.

TABLE III
THD FOR DIFFERENT LOAD CONDITIONS

Load	THD with FCS-MPC	THD with PI
20%	9.64%	15.15%
40%	4.87%	9.32%
60%	4.77%	7.23%
80%	4.16%	6.29%
100%	4.07%	6.06%
120%	4.36%	6.26%

Both active PFC fulfilled the norm, as seen in Fig. 6 and Fig. 10 (even in higher harmonics that are not seen in these figures). However, there are some peculiarities that needs

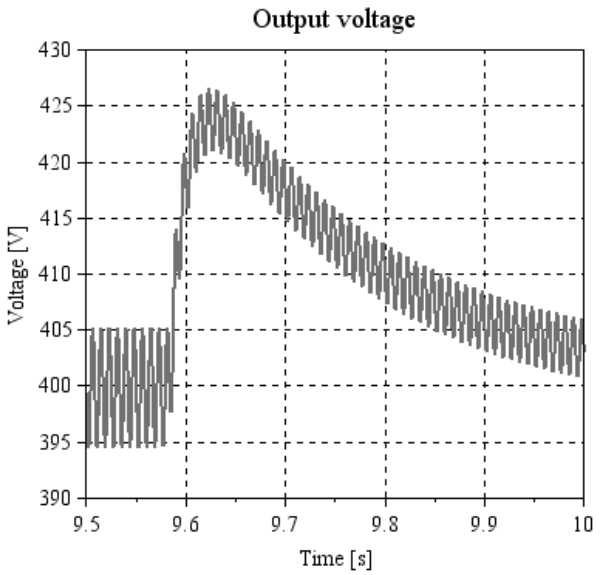

Fig. 12. Voltage transient with load disturbance with PI in internal loop

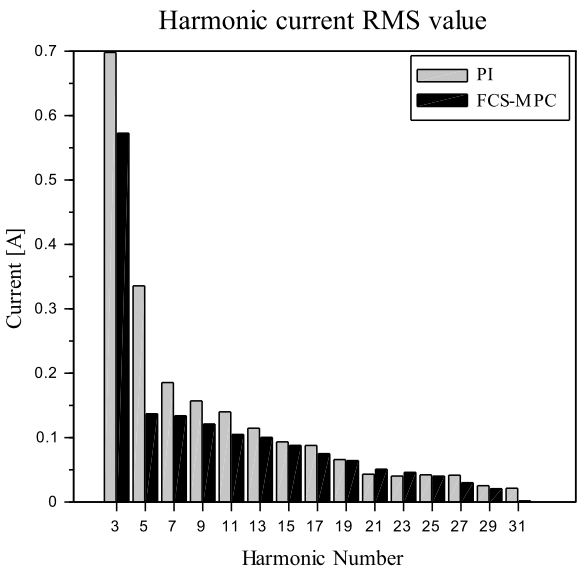

Fig. 14. Harmonic currents comparison between PI controller and MPC

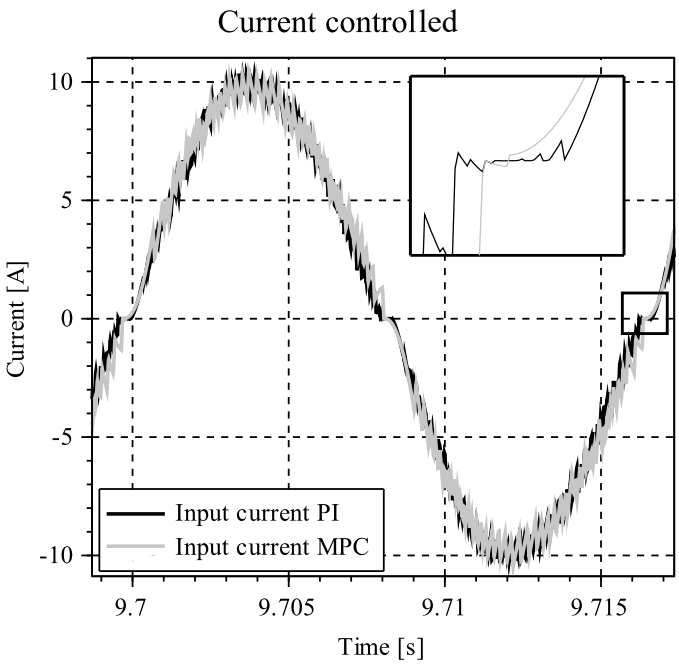

Fig. 13. Source current comparison (zero crossover in detail)

highlights:

- Besides the PFC design with MPC were made for THD = 3%, the obtained result at rated operation can be considered satisfactory (see Table III). Obviously, there is some distortion in the own current reference, since there is some influence of voltage loop. Considering only the current loop, the results are agreeing with the project.
- The same occurs with project for PFC with PI current control: the external voltage loop reduces the quality of the results, although the result still is in agreement with the international standard.
- Compared directly one with other (Fig. 14), MPC presented lower harmonic current amplitude for low harmonics while PI had some lower harmonic current amplitude for some of high harmonics. Overall, MPC had lower individual harmonics, which explains the lower THD than the PI.
- The voltage loop with PI current controller in internal loop is faster than the voltage loop with MPC current controller in internal loop. This way, in the load disturbance, the first had lower voltage peak (6,5% – see Fig. 12) than the second (9,0% – see Fig. 8). To improve this results, it is necessary to use a higher cut-off frequency in the control design. However, as faster the voltage loop is, worst the current THD will be. Note that the voltage ripple, in both conditions were the same (1.25%), as predicted in converter design (both converters were designed for 1.5-2.0% voltage ripple).
- Analyzing Fig. 7 and Fig. 11, the fundamental frequency of command signal (despite the DC level) is the 120 Hz, used to tracking the current reference (see Fig. 5 and Fig. 9). However, in the PI command, frequencies at almost 10 kHz and 20 kHz are distinct in the harmonic spectra, since there are a fixed operation frequency. In the MPC command, operation frequency is limited to 20 kHz of sampling frequency, but it is a variable frequency. Therefore, this control acts in the frequency it needs to act at each moment. It is interesting that the frequency grows to track the peak of the current reference and reduces to track the reference in low values.
- The current ripple with PI current controller is considerably lower than with the MPC current controller. Since PI operates in a high fixed frequency, the inductor is

capable to filter the higher harmonics caused by switching frequency. As the MPC frequency is lower, the current ripple is higher since the inductor do not filter these low frequencies. Otherwise, in the converter design with PI current controller, the inductor was designed considering the current ripple. In the converter design with MPC current controller, the inductor was designed considering the input current THD. It explains why the MPC has lower THD even with higher current ripple. Notably, in the zero point of the reference, with PI current controller, there is a current dead zone, which also reduces the THD. With MPC controller tracking the reference, this effect is attenuated, which improves the THD (as seen in Fig. 13).

- The boost converter with MPC current control used a lower output filter for the same voltage ripple. In other hand, the boost converter with PI used a lower inductance than the MPC and gives lower current ripple, besides the higher THD.
- Both controllers presented lower THD even in low load condition. It explains the advantage of active PFC in relation to passive PFC, independently of the employed technique.

VII. Conclusion

This work presented a design methodology for active PFC with FCS-MPC current controller. The design was evaluated and compared with a conventional PI current controller solution for active PFC with boost converter.

The presented design methodology uses two abacus for design the inductance and the capacitance of boost converter, considering a predictive current control. For voltage control design, the use of a numerically identified model was considered. The methodology shows itself valid, since the final THD was near to expected in the project.

The comparison with PI controller showed the differences between both techniques. As PI operates with fixed switching frequency, the current ripple with this technique is lower, but it is incapable to lead with zero points of current reference which reduced it THD (associated to this fact is the faster voltage loop, which causes some distortion in current reference). This way, the predictive controller presented lower THD, at rated operation and in any other tested load condition if compared with PI.

The active PFC techniques are a reliable solution for equipment with non controlled rectifiers in input stage and need to fulfill international standards. The presented techniques were capable to fulfilled the IEC 61000-3-2 standard and have high power factor, allowing better use of industrial electric grids, with these equipment.

For futures works, it is suggested to explore FCS-MPC with higher prediction horizons, to compare the finite control set technique with continuous control set MPC techniques and to test the capability of MPC techniques in constraints treatment.

References

[1] *Electromagnetic compatibility (EMC) Part 3-2: Limits - Limits for harmonic current emissions (equipment input current $\leq$16 A per phase)*, IEC61000-3-2 Std., 2005.

[2] L. Roggia, J. E. Baggio, and J. R. Pinheiro, "Predictive current controller for a power factor correction boost converter operating in mixed conduction mode," in *13th European Conference on Power Electronics and Applications, 2009. EPE 09.*, 2009, pp. 1–10.

[3] S. Wall and R. Jackson, "Fast controller design for single-phase power-factor correction systems," *IEEE Transactions on Industrial Electronics*, vol. 44, no. 5, pp. 654–660, Oct 1997.

[4] L. Roggia, F. Beltrame, J. E. Baggio, and J. R. Pinheiro, "Digital current controllers applied to the boost power factor correction converter with load variation," *IET Power Electronics*, vol. 5, no. 5, pp. 532 – 541, 2012.

[5] S. Vazquez, J. Leon, L. Franquelo, J. Rodriguez, H. Young, A. Marquez, and P. Zanchetta, "Model predictive control: A review of its applications in power electronics," *IEEE Industrial Electronics Magazine*, vol. 8, no. 1, pp. 16–31, Março 2014.

[6] A. Bouafassa, L. Rahmani, B. Babes, and R. Bayindir, "Experimental design of a finite state model predictive control for improving power factor of boost rectifier," in *2015 IEEE 15th International Conference on Environment and Electrical Engineering (EEEIC)*, 2015, pp. 1556 – 1561.

[7] C. Bordons and C. Montero, "Basic principles of mpc for power converters: Bridging the gap between theory and practice," *IEEE Industrial Electronics Magazine*, vol. 9, no. 3, pp. 31–43, Setembro 2015.

[8] Y. Geng, Y. Liu, J. Chen, and P. Luo, "Analysis and design of a predictive ccm power factor correction converter," in *2013 International Conference on Communications, Circuits and Systems (ICCCAS)*, 2013, pp. 398 – 401.

[9] M. Abedi, B.-M. Song, and B. Ernzen, "Optimum tracking of nonlinear-model predictive control for boost based pfc rectifier," in *2011 IEEE 43rd Southeastern Symposium on System Theory*, 2011, pp. 87–91.

[10] M. Yazdanian, S. Farhangi, and M. R. Zolghadri, "A novel control strategy for power factor corrections based on predictive algorithm," in *2010 1st Power Electronic & Drive Systems & Technologies Conference (PEDSTC)*, 2010, pp. 117–121.

[11] S. J. Qin and T. A. Badgwell, "A survey of industrial model predictive control technology," *Control Engineering Practice*, vol. 11, pp. 733–764, 2003.

[12] D. Q. Mayne, "Model predictive control: Recent developments and future promise," *Automatica*, vol. 50, pp. 2967–2986, November 2014.

[13] H. Young, M. Perez, J. Rodriguez, and H. Abu-Rub, "Assessing finite-control-set model predictive control," *IEEE Industrial Electronics Magazine*, vol. 8, no. 1, pp. 44–52, March 2014.

[14] G. Negri, M. Bartsch, .A.G.and Cavalca, J. de Oliveira, A. Nied, and A. Silveira, "Model-based predictive direct speed control applied to a permanent magnet synchronous motor with trapezoidal back-emf," in *2014 11th IEEE/IAS International Conference on Industry Applications (INDUSCON)*, 2014.